PHOTOGRAPHIC OBSERVATIONS ON FATIGUE FRACTURE OF POLYCARBONATE

HIGUCHI, Masakazu
Research Institute for Applied Mechanics, Kyushu University : Professor

ISHII, Hideo
Research Institute for Applied Mechanics, Kyushu University

https://doi.org/10.5109/7168664

出版情報：Reports of Research Institute for Applied Mechanics. 16 (53), pp.69-96, 1968. 九州大学応用力学研究所
バージョン：
権利関係：

Reports of Research Institute for Applied Mechanics
Vol. XVI, No. 53, 1968

PHOTOGRAPHIC OBSERVATIONS ON FATIGUE FRACTURE OF POLYCARBONATE*

Masakazu HIGUCHI** and Hideo ISHII***

Synopsis

Experiments of fatigue fracture were carried out at slow speeds of repetition of 1 c/sec or lower with the specimens heat-treated at 140°C for the purpose of pre-conditioning together with annealing. It has confirmed the existence of the transition of the fatigue fracture mode from of a shear-type to of a tension-type, and revealed that the stress of the transition depends on the ratio between the shearing and tensile stress components.

The shear-type cracks also appear near below the transition earlier than the tension-type ones do, to be outstripped. There are very often observed plastically deformed zones on the tension-type fracture faces well below the yield stress of the material, which accompany numerous microscopic deformation bands derived from many of fine crazes on the specimen surfaces. Although the appearance of the fracture crack is zigzag in such a case, the primary crack is planar in the inside of the specimen.

1 Introduction

Polycarbonate has a transition of its fracture mode when subjected to stress repetitions[1], depending on the magnitude of the stress. In addition, it has other interesting properties. Deformation bands**** appear under tension as well as under torsion. It is likely that the appearance of deformation bands can be called yielding. It occurs at a statical tension test just after a decrease in load which is due to a mechanical instability which ought to be distinguished from yielding[2]. In torsion, however, the mechanical instability is likely to occur on account of yielding. Under cyclic stresses, on the other hand, deformation bands are produced well below the yield stress. Above all the material increases in rigidity with the repetition of stress in the early stage of fatigue[3].

We are interested especially in the similarity of these properties to those of mild steel, though such thermoplastic materials as polycarbonate are in no doubt

---

* This article is based on part of a paper presented at the meeting of JSME held in Fukuoka on March 1, 1968.
** Professor, Member of the Research Institute for Applied Mechanics, Kyushu University.
*** Research Institute for Applied Mechanics, Kyushu University.
**** Thanks are due to Professor A. S. Argon who first drew our attention to these bands.

much affected by the heat which will generate on stress repeating.

The present work is the results of the observation made in the course of studying on the mechanism of fatigue at room temperature, at present apart from getting practical data.

2. Materials and method of measurement

The specimens used were prepared from plates and bars of phosgenation process-produced polycarbonate on the market. Its molecular weight was about 30,000. After turning or shaping, finally the materials were buffed mirror smooth with alumina powder-holding wett felt. They might have a variety of residual stresses on account of the difference of storage conditions and minor variations in the course of specimen preparation. They were heat-treated for 5 hours in the bath of silicone oil at 140 ℃ and cooled at a rate of 0.1 ℃/min in the bath, with reference to the measurements[4] of the decrease in the residual stresses and the increase in distortion of the specimens with the rise of annealing temperature (Figs. 1 and 2); the temperature is not high enough to anneal the materials as seen from the data but a compromise between the stress removing and specimen warping. We made such treatment for the purpose of a sort of pre-conditioning for our experiments.

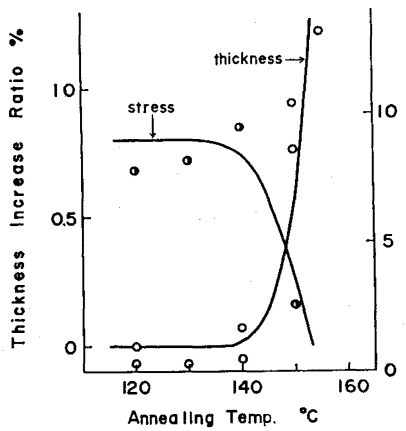

Fig. 1. Maximum residual stress reduction and heat distortion increase with annealing temperature (reproduced from Ref. 4)

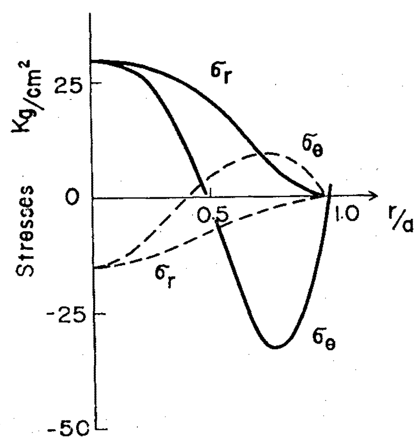

Fig. 2. Residual stresses of a rod material (reproduced from Ref. 4)
—— as received
a, r radius and distance from center
…… annealed
σ_θ, σ_r hoop and radial stress

The specimen surfaces thus prepared showed rather rough under a microscope (Fig. 4) and it resulted from the very annealing. They were not repolished.

The surfaces seemed, however, less notch-sensitive than when they were, not annealed, smooth enough in appearance and had a few faint scratches left. This is our another compromise between minimizing of data scattering and economy of labor for specimen preparation. A specimen thus prepared had a value of 220 kg/mm² of Young's modulus under tension at a straining rate of 1.2×10^{-5}/sec, and an ultimate tensile nominal stress of 6.79 kg/mm².

Fatigue testing machines of a Schenck type and of an Ono type were used in the condition of completely reversed stress repeating at a reduced speed of about 60 cycles per minute. An Instron-type (Shinko-Tom 5,000) and a Rhiele-type (Shimadzu-RT 50) machine were used respectively for fluctuating tensile (minimum load and maximum load both tensile) and fluctuating torsional stresses at rates as low as 2.5 cycles per minute. These slow rates of stress repetition were selected to reduce the temperature rise of the specimens.

The air of the room was regulated as 23 ± 1.1 ℃ and $50 \pm 3\%$ RH.

3. Two modes of fatigue fracture

Fatigue fracture shows a transition of the mode from a tension- to a shear-type at a shear strain of 0.04 or so (about 3 kg/mm² of shear stress) for our material (Fig. 3) when subjected to torsion. At higher stresses the fracture occurs as shown in Figs. 5a and 5b at the mid length of the specimens even when there is no stress concentration. It is presumably owing to a higher temperature caused by poor conduction of heat of the material.

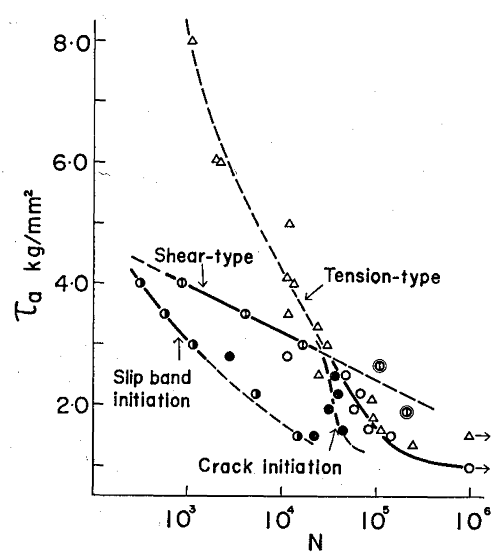

Fig. 3. SN-curves
△ Rotating bending
○⦶ Reversed torsion
◎ Ditto, but with a groove at periphery

The specimens, warming up with the stress repetitions and thermally expanding under the condition of fixed ends, bulge out at the mid length, the softer portion at a higher temperature. On the other hand, the softness brings about the strain concentration which is accompanied by generation of the more heat. The extent of the soft part can be distinctly demarcated (Fig. 6b) and it will be because the softening and the strain concentration become the cause of each other. Prior to occuring of the local strain increase, slip bands appear in both longitudinal and circumferential directions as seen in Fig. 6a. One can see the appearance of the bands, the concentration of strain, and the final state of the fracture region in Figs. 6a through 6c. The fine numerous slip bands close to whitish protrusions and the hazy circumferential zone adjacent the protruded region are perceptible in Fig. 5b.

Near below the transition, one or more shear-type cracks of small size first appear in places. But later one or two tension-type cracks appear somewhere else in the repetitions denoted 'crack initiation' in Fig. 3 and one of them rapidly grows to fracture. Figs. 7 through 9 show some of tension-type cracks, the last of which has a fracture surface being made up of tensile stress- as well as shear stress-broken parts.

A few specimens with a circumferential groove were used. Their cracks were observed to run circumferentially under the stresses below the transition, but with reluctance; they had been continually checked from changing over to shear-type cracks (Figs. 10a and 10b). At a little smaller stress a crack of tension-type was sure to grow indifferently to the groove (Fig. 10c). The data for the circumferential cracks were plotted with the approximate values of stresses evaluated from the theory of elasticity, and were revealed to lie on the extended part of the life line of shear-type fracture (Fig. 3). On the contrary, the tension-type fracture is obtained above the transition when the specimen is subjected to rotary bending, in which case the shear stress is half the tensile stress in magnitude and the shear-type fracture line is expected to shift upward to double the ordinates. In other words, there may be found a transition beyond 7 kg/mm^2 of tensile stress, the value at which the material yields.

Such as in Fig. 11 is another appearance of the shear-type cracks and was obtained with a not annealed specimen. Thin filamentous materials, rolling to and fro with the alternation of twist, were squeezed out from closely running shear cracks. There was another case in which such a crack arose in the direction of the axis of an annealed specimen.

4. **Fatigue fracture due to tensile stress**

Figs. 12 through 13c show a crack on a specimen of a 2 mm thick hollow cylinder of 20 mm diameter. The specimen was twisted repeatedly between such angles that neither the maximum stress passes the transition nor the minimum goes down to zero. The crack ran at an angle of about 50°, measured after removing the load, to the specimen axis to make a helix. The value of the angle

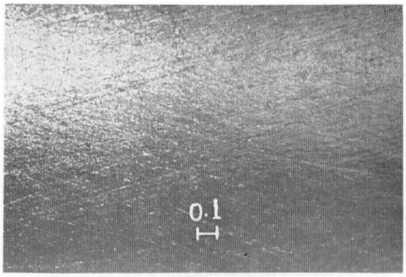

Fig. 4. Annealed specimen surface ready to fatigue test
— 0.1 mm

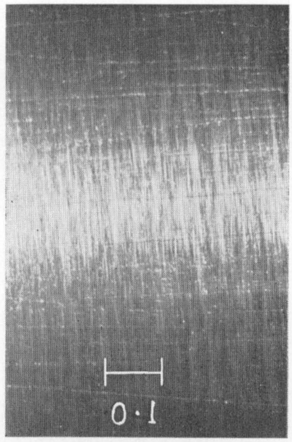

Fig. 6a. Deformation bands, longitudinal and circumferential

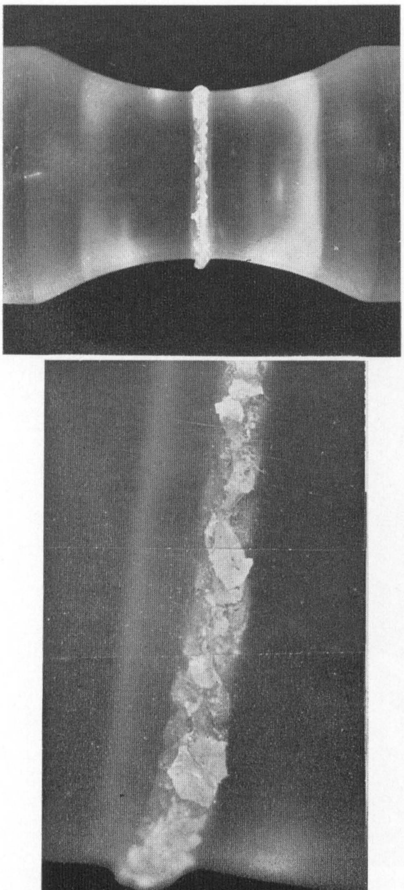

Figs. 5a, b. Shear-type fractures

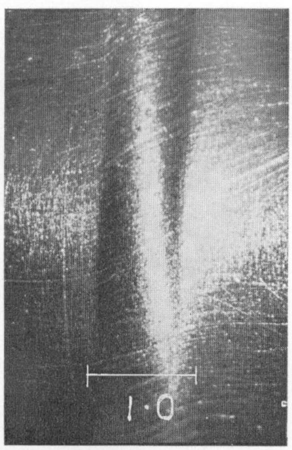

Fig. 6b. Buldging out accompanying with shear strain concentration

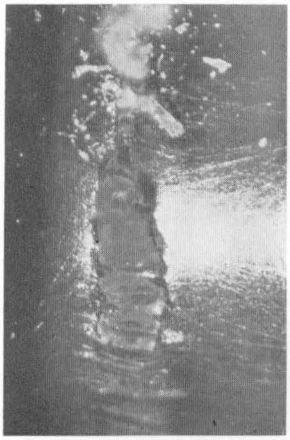

Fig. 6c. Close up of shear-type fracture

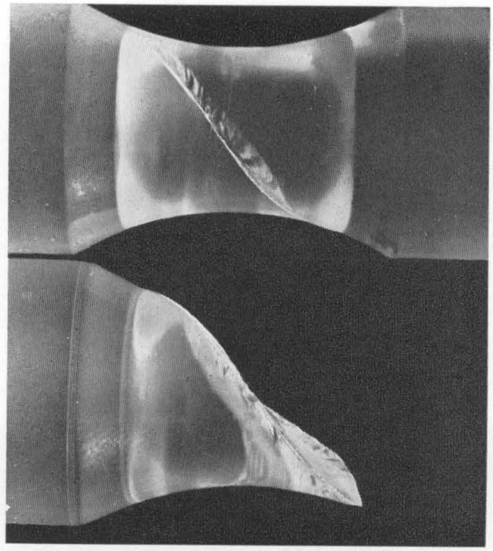

Fig. 7a. Tension-type fracture
Fig. 7b. Tension-type fracture for a specimen with a lateral hole

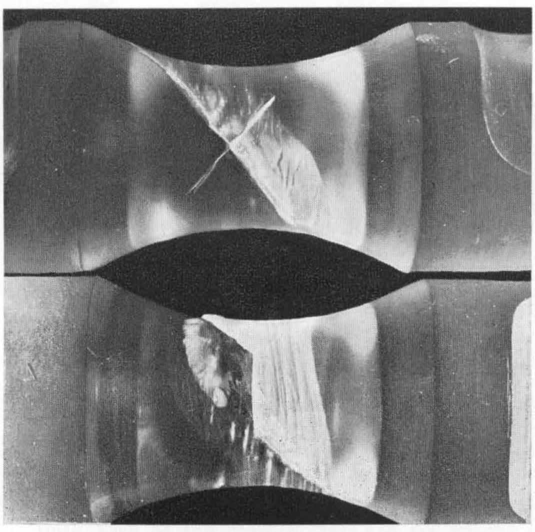

Fig. 8. Double cracks
Fig. 9. Jointly appearing of both types

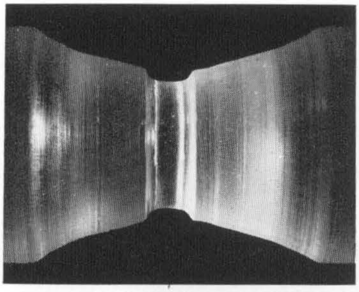

Fig. 10a.

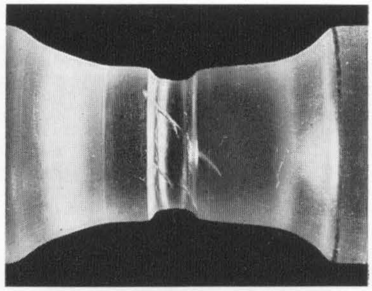

Fig. 10c.

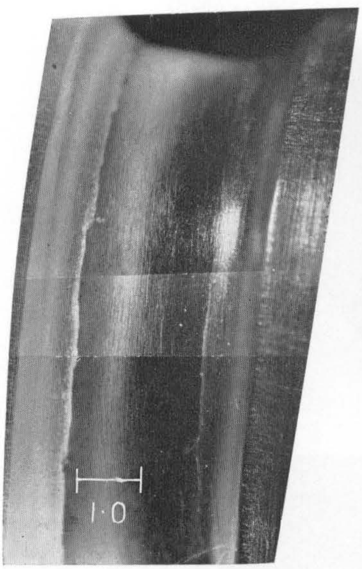

Fig. 10b.

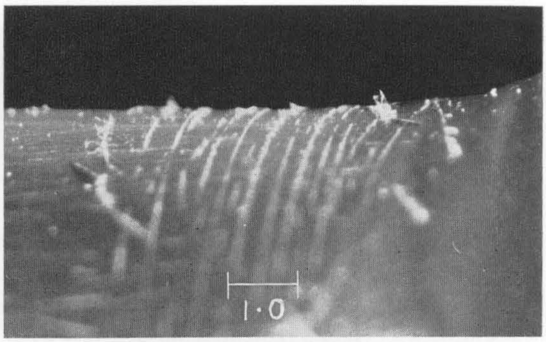

Fig. 11.

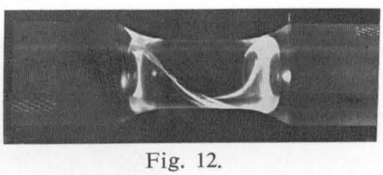

Fig. 12.

Figs. 10a, b. Shear-type crack below transition and its close up view

Fig. 10c. Tension-type crack outgrowing shear-type crack below transition

Fig. 11. Shear-type sharp cracks

Fig. 12. Tension-type helical fracture of a hollow cylindrical specimen
Both ends of the parallel part are not cracks but reflection of light.

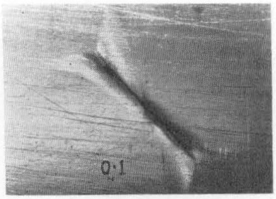

Fig. 13a.

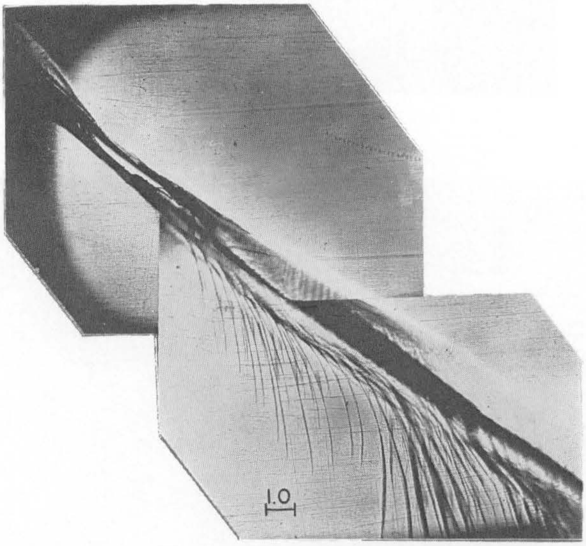

Fig. 13b.

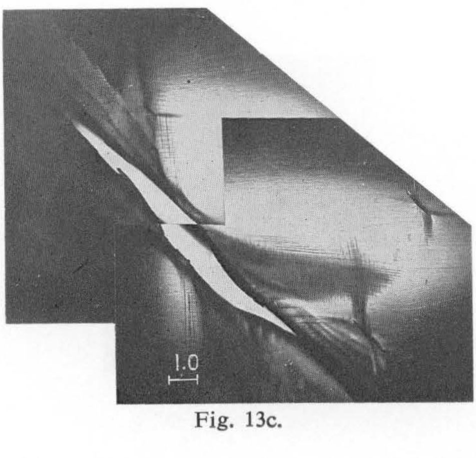

Fig. 13c.

Figs. 13a, b, c. From birth of a tension-type crack to fracture
Note the deformation bands by the crack.

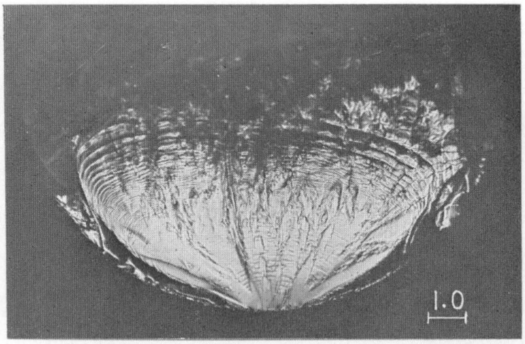

Fig. 14a.

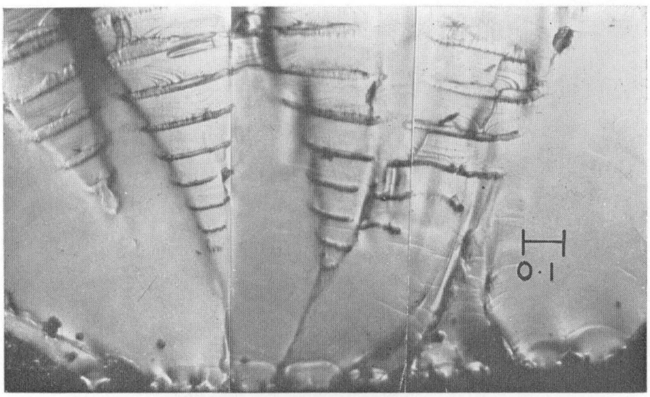

Fig. 14b.

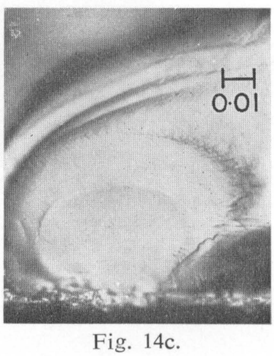

Fig. 14c.

Figs. 14a, b, c. Tension-type fracture under rotating bending
The latter two shows a nucleus; its under edge is a craze zone.

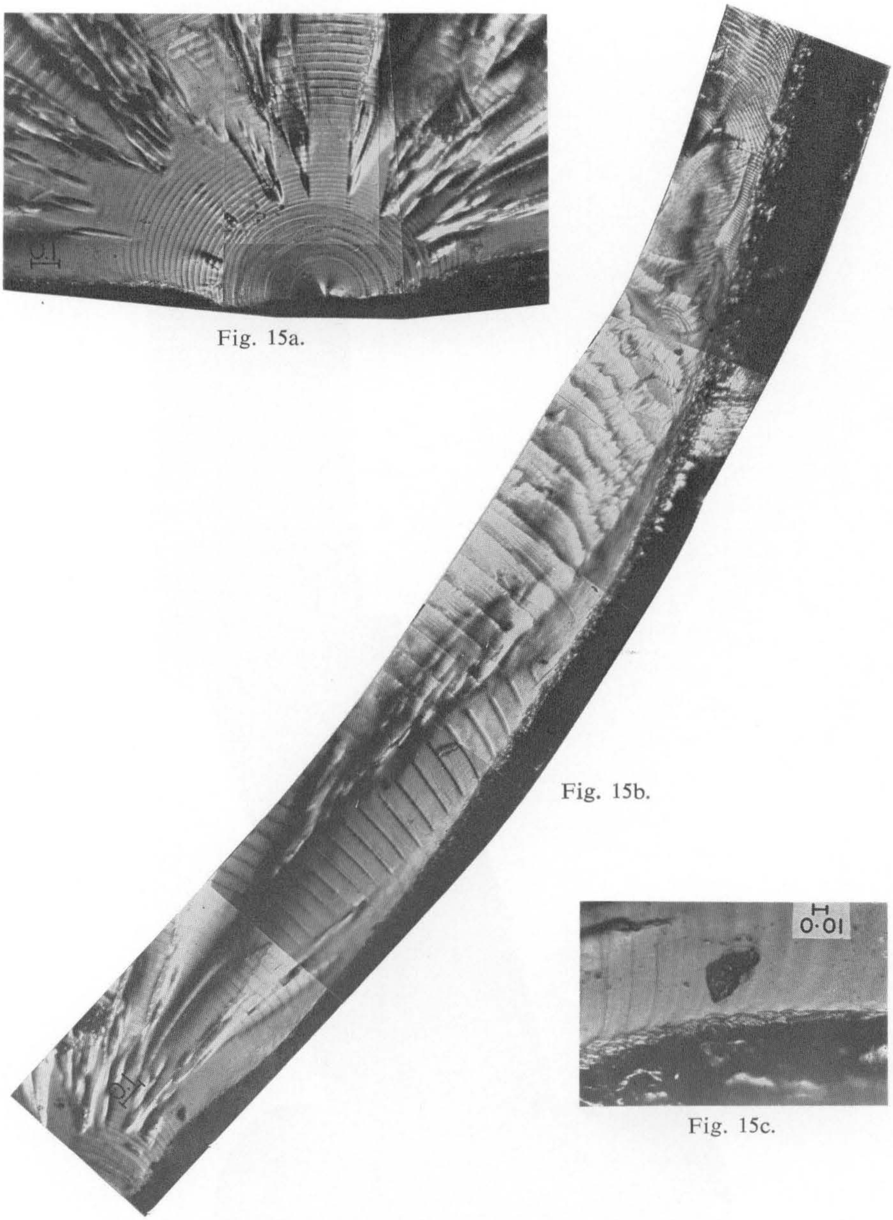

Fig. 15a.

Fig. 15b.

Fig. 15c.

Figs. 15a, b, c. Another fracture due to rotating bending, showing typical striations Dark area in *c* (lower half) shear zone on the periphery, magnified

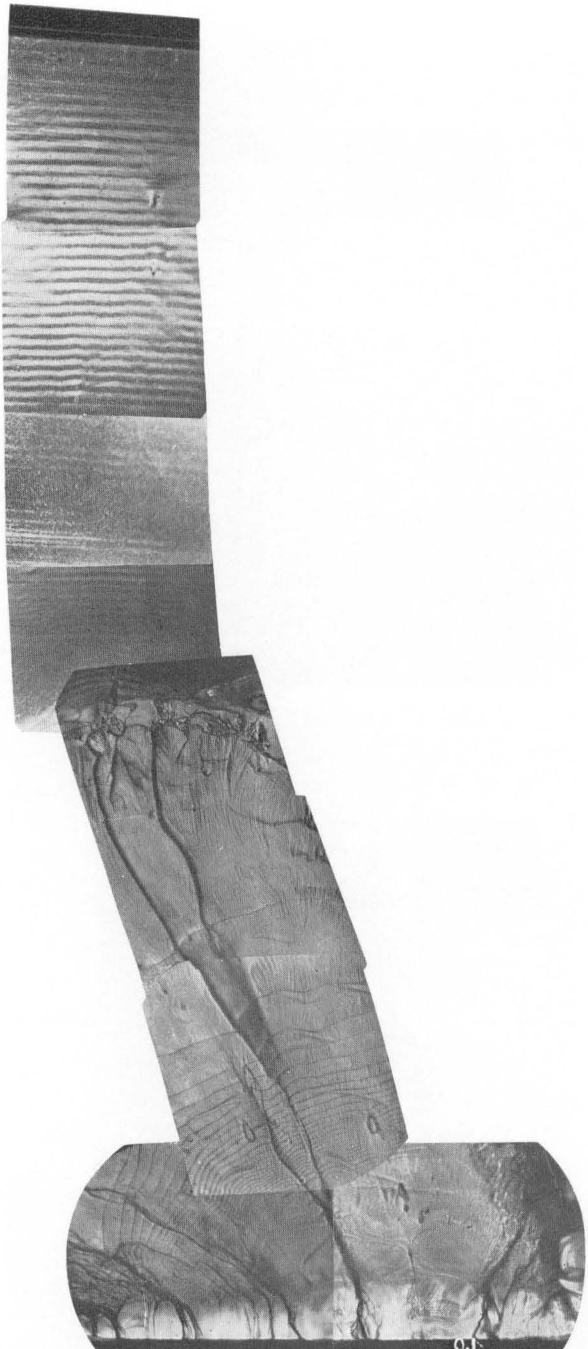

Fig. 16. Fracture under fluctuating tension
Bottom edge craze zone (whitish)
Upper half catastrophic break region accompanying Wallner lines

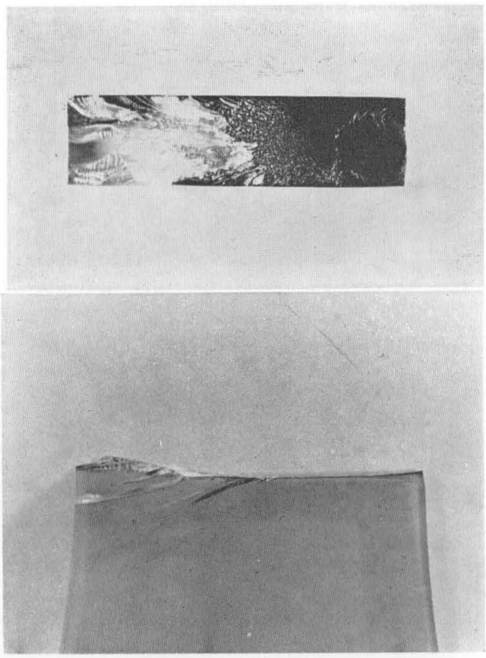

Fig. 17a.

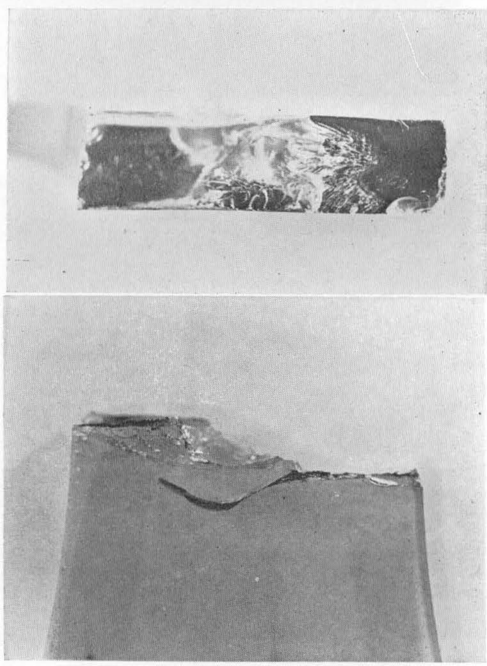

Fig. 17b

Fig. 17. Specimens broken under fluctuating tension
Stress ranges are $2.51 \sim 1.33$ and
$3.45 \sim 2.55$ kg/mm^2 respectively.

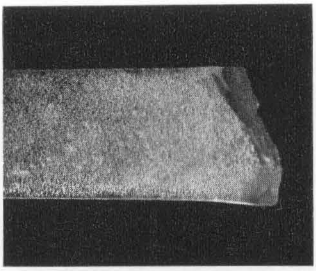

Fig. 18a. Numerous crazes produced perpendicularly to stress direction

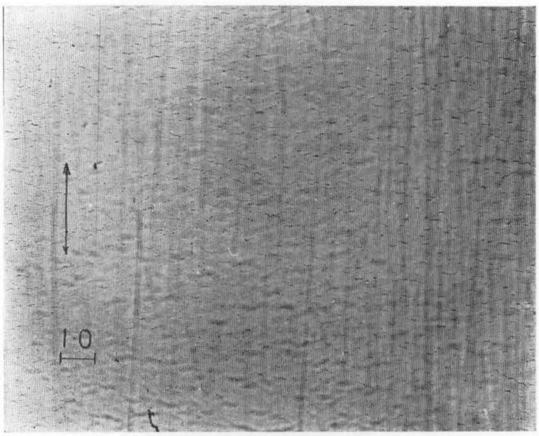

Fig. 18b.

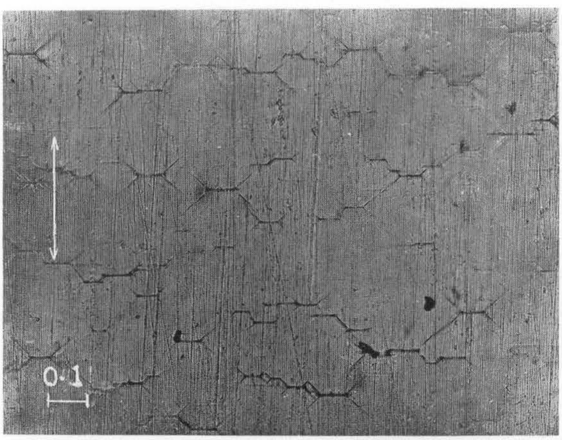

Fig. 18c.

Figs. 18b, c. Close up of crazes and deformation bands at each of craze ends

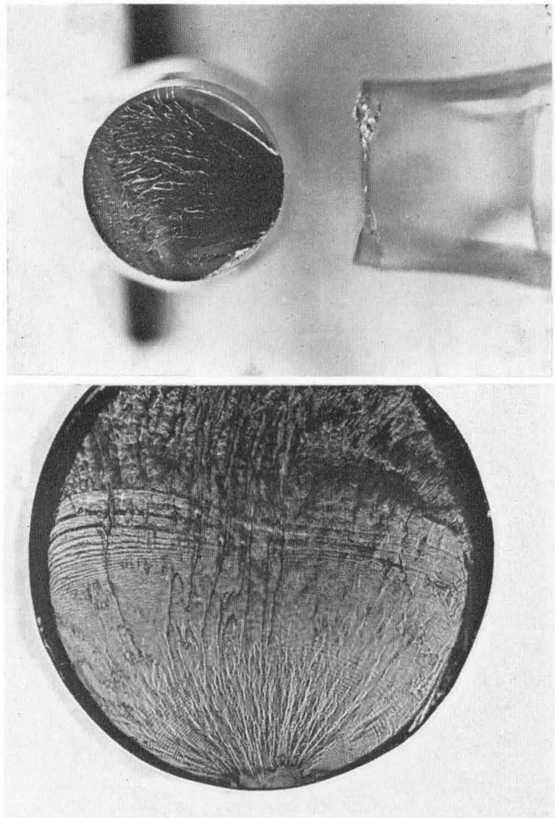

Fig. 19. Necking zone hemming tension-type fracture zone in rotating bending

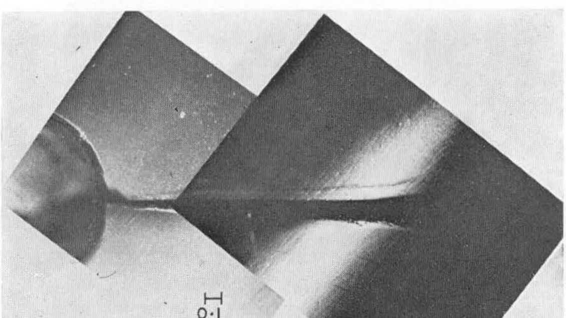

Fig. 20a. A crack originated at a hole together with a shear zone as a radial dull line

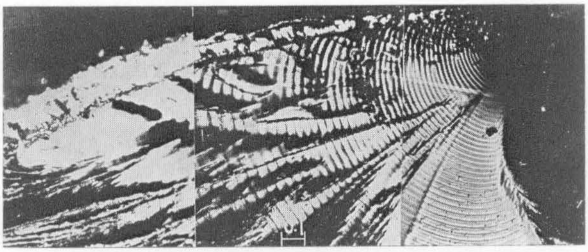

Fig. 20b. Fracture face of the crack of Fig. 20a
Shear fracture zone is seen on the upper rim.

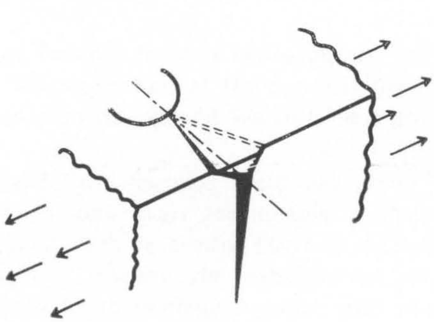

Fig. 20c. Formation of a shear lip

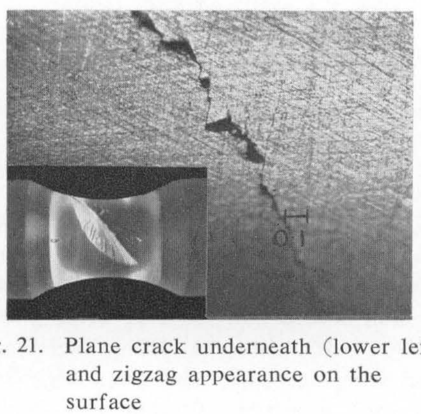

Fig. 21. Plane crack underneath (lower left) and zigzag appearance on the surface

may have an error due to unloading. But it is below 1°∼2°, dependent on the strain. In Fig. 13a, one can see the crack growing accompanied by slip bands formation on both sides of the crack; the bands are found close fine lines (Figs. 13b, c) and ones on one side make an angle larger than 90° with those on the other side after removing the load (Fig. 13a).

Figs. 14a through 15c show the fracture faces of specimens subjected to rotating bending in which the processes of fracture from a craze to a crack nucleus and to crack growth with striations are observed. The pitch of the striations increased with the crack growth. There appeared in the intermediate zone other faint striations with a small pitch between the primary ones. The secondary ones merge imperceptibly into the primary after growing up. The number of striations after the middle stage was likely to accord with that of stress repetitions. Some of striations were measured by an optical section method to be 1∼2 μm high on both faces.

The feature of the fracture faces is again shown in Fig. 16 for the case of fluctuating tensions. The upper half of the figure is the final part of catastrophic break. There are seen regularly spaced Wallner lines produced by elastic waves, not striations.

Other tensile stress fatigue fracture faces are given in Fig. 17 in order to show that the fracture in some cases accompanies a little of necking. Note the part near the top right of each specimen. There is a crack initiation at the mid width and its development toward the surroundings on the specimen. Badly done neckings were brought about there together with rough striations when the fracture developed to both the side surfaces, and made the fracture face slanting. Many of crazes, produced perpendicularly to the stress direction on the specimen surface, and as many deformation bands, developing out of the craze ends at an angle of about 35° with them, made such ductility possible to show up in fatigue (Figs. 18a through 18c). Similar necking zones are seen in Fig. 19 on the periphery of the fracture face.

5. The shear fracture zone hemming the tension-type fracture face

The shear-type fracture on such a zone goes behind the primary one and retards its propagation along the adjoining region, probably because the energy to break is more in shear-type fracture than in tension-type one. Peculiarities observed in growing of a tension-type crack under repeating shear stress are revealed with this understanding of the accompanying shear-type fracture.

A fracture which originated at a halfway drilled hole on a specimen surface is shown in Fig. 20a, and in Fig. 20b in which the hole appears as half a U-shaped dark area at the right hand side. A shear zone increases in width with crack growth from the origin to the left. It has a form such as shown in Fig. 20c. The primary crack, which makes an angle about 50° with the axis of torsion, growing faster, gets under the surface. Prior to break and after plane strain deformation, the remaining surface layer as thin as 0.1 mm contiguous the crack edge develops deformation bands extending in both directions from the edge of the primary crack. Break of the shear zone is a process of joining of shear-type cracks running at a nearly right angle with each other, and appears zigzag (Fig. 21).

6. Conclusion

Plates and bars of phosgenation process-produced polycarbonate on the market have a fracture-mode transition at a strain of 0.04 (about 3 kg/mm^2 of stress) when they are heat-treated at a temperature 140 ℃.

The super-transitional fracture pertains to the magnitude of the shear strain or stress component and the sub-transitional one to that of the tensile component, and accordingly the transition depends on the ratio of both components.

The cracks of both types jointly or separately appear in the neighborhood of the transition. In those cases, the tension-type crack, coming later, grows faster and leads the specimen to break.

Very often the tension-type fracture includes the shear-type fracture zone in it, which is adjacent to the specimen surface. Accordingly the crack is made to grow zigzag on the surface. But the tension-type crack, getting under the surface about 0.1 mm deep, develops in the inside and makes a plane of primary fracture, with the striations rising $1\sim2\,\mu m$ high.

References

1) S. Hori, Kikai no Kenkyu, 11, 5 (1959).
2) M. Higuchi, H. Hyakutake, Preprint of JSME Kyushu Branch Meeting, No. 68-2, 53, March 1, 1968, and Rep. Research Institute for Applied Mechanics, 16, 54, (1968).
3) M. Higuchi, H. Ishii, Rep. Research Institute for Applied Mechanics, 16, 53, (1968).
4) H. Hyakutake, Proc. 11th Japan Congress on Materials Research, 164 (1968).

(Received July 6, 1968)